J Solid State Electrochem (2008) 12:643–649
DOI 10.1007/s10008-007-0334-0

ORIGINAL PAPER

Pt–Fe cathode catalysts to improve the oxygen reduction reaction and methanol tolerance in direct methanol fuel cells

A. M. Castro Luna · A. Bonesi · W. E. Triaca · V. Baglio · V. Antonucci · A. S. Aricò

Received: 28 July 2006 / Revised: 26 August 2006 / Accepted: 14 September 2006 / Published online: 22 May 2007

Abstract High surface area carbon-supported Pt and bimetallic Pt–Fe catalysts are investigated for the oxygen electroreduction reaction (ORR) in low-temperature direct methanol fuel cells (60 °C). The electrocatalysts are prepared using a combination of colloidal and incipient wetness methods allowing the synthesis of carbon-supported bimetallic nanoparticles with a particle size of about 2–3 nm. These materials are studied in terms of structure, morphology and composition using X-ray diffraction, X-ray fluorescence and transmission electron microscopy techniques. The electrocatalytic behaviour of these catalysts for ORR is investigated by employing the rotating disc technique. An enhancement of the ORR is observed with the bimetallic Pt–Fe catalyst in the oxygen-saturated electrolyte solution, with and without methanol.

Keywords Binary platinum-based metal alloy · Methanol crossover · Fuel cell

Dedicated to Prof. Dr. Teresa Iwasita on the occasion of her 65th birthday in recognition of her numerous contributions to interfacial electrochemistry.

A. M. Castro Luna (✉) · A. Bonesi · W. E. Triaca
INIFTA, Universidad Nacional de La Plata,
Suc.4, CC 16 (1900),
La Plata, Argentina
e-mail: castrolu@inifta.unlp.edu.ar

V. Baglio · V. Antonucci · A. S. Aricò
CNR-ITAE,
Via Salita S. Lucia sopra Contesse,
5-98126 Messina, Italy

Introduction

One of the most promising applications of direct methanol fuel cells (DMFCs) is related to the field of portable power sources [1, 2]. At present, there are still some challenging research targets to commercialise DMFCs in the power sources market: (1) to develop new polymer electrolyte membranes with high proton conductivity and low methanol crossover, (2) to find novel anode catalysts with improved electrode kinetics for the methanol electro-oxidation reaction and (3) to develop cathode catalysts with high activity towards the oxygen reduction reaction and suitable tolerance to methanol.

Methanol crossover results in a significant loss in voltage efficiency of a DMFC because on the commonly used Pt/C cathode catalyst, methanol would be oxidised competing with O_2 reduction. To avoid this problem, one approach is the use of an oxygen reduction catalyst that is inactive towards methanol oxidation or with a high methanol tolerance. Thus, it is necessary to develop novel Pt-based electrocatalysts that are able to catalyse oxygen reduction but limit the oxidation of methanol.

Many investigations have shown that some binary Pt-based alloy catalysts, such as Pt–M, (where M=Co, Cr, Fe), exhibited an enhanced electrocatalytic activity for the ORR in comparison with Pt alone [3–5]. The activity enhancement was explained by the increased Pt d-band vacancy (electronic factor) [6] and by the favourable Pt–Pt interatomic distance (geometric effect) [7].

One concern with Pt alloys in fuel cells is the dissolution of transition metals. Pourbaix diagrams indicate that most transition metals such as Co, Cu, Fe, Cu, etc. are soluble at a potential between 0.3 and 1 V versus SHE and at pH=0 [8]. In this respect, Toda et al. [9] reported that after electrochemical testing with Pt–Fe

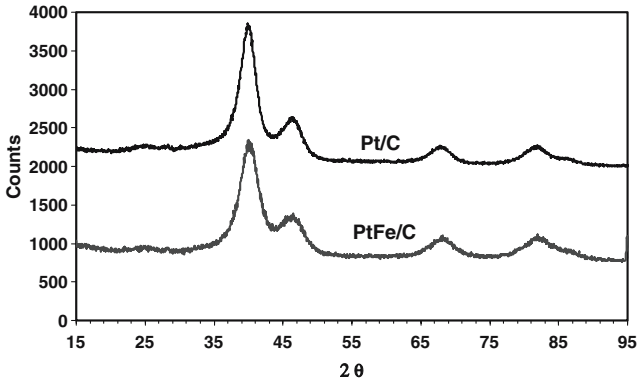

Fig. 1 XRD patterns of Pt/C and PtFe/C catalysts

alloy, the catalyst was covered by a thin Pt skin of less than 1-nm thickness.

Most of the previous studies have dealt with catalysts characterised by a particle size larger than 4 nm and low concentration of active phase on carbon due to the need of high-temperature treatment to form bimetallic alloys of transition metals with Pt [4, 10–12]. However, to accelerate the oxygen reduction process, a suitable number of surface sites is necessary. Moreover, various studies have indicated that for supported Pt/C catalysts, a maximum catalytic activity occurs at about 3 nm as an appropriate compromise between the number of active sites and crystallographic phases with low Miller indices characterised by high intrinsic activity [13–15]. To synthesise a highly dispersed electrocatalyst phase in conjunction with a high metal loading on a carbon support is one of the present goals in DMFC development. In this respect, we have employed a new methodology to get small bimetallic carbon-supported particles [16].

The aim of this work was to evaluate the electrocatalytic activity towards the ORR, together with the methanol tolerance characteristics of the novel synthesised supported catalysts.

Materials and methods

Preparation and characterisation of the catalysts

Platinised carbon was prepared by using the sulphite-complex route [17]. A $Na_6Pt(SO_3)_4$ precursor was obtained from chloroplatinic acid. A Vulcan XC-72R carbon black was suspended in distilled water and agitated in an ultrasonic water bath at about 80 °C to form a slurry. A proper amount of $Na_6Pt(SO_3)_4$ was successively added to the slurry. The Pt sulphite complex solution was decomposed by adding H_2O_2 to form colloidal PtOx/C. Subsequently, 60% Pt/C was obtained by reducing the PtOx/C in a H_2/He stream. A 60 wt% PtFe/C with a catalyst atomic composition Pt_3Me_1 was prepared starting from PtOx/C. To prepare the 60 wt% Pt–Fe/C catalyst, an impregnation procedure was employed. The bimetallic catalysts were reduced in a H_2 stream at room temperature.

All materials were studied in terms of structure, morphology, composition and surface chemistry using X-ray fluorescence analysis (XRF), powder X-ray diffraction (XRD) pattern and transmission electron microscopy (TEM).

The Pt/M atomic ratio was determined in the samples by XRF; from XRD patterns, the peak profile of the (220) reflection in the face-centred cubic structure was obtained using the Marquardt algorithm and used to calculate the crystallite size using the Debye–Sherrer equation.

Electrochemical measurements

Rotating disc electrode

The rotating disc technique was employed to study the ORR on the cathode catalysts. The rotating disc electrode consisted of a glassy carbon rod (0.125 cm^2 geometric area) covered by a thin layer of catalyst, with a metal loading of 14 $\mu g/cm^2$ imbedded in a Nafion® polymer electrolyte film of 0.1 μm [18].

A standard three-electrode cell was employed to electrochemically characterise the supported catalyst materials. The rotating disc was employed as working electrode, a Pt foil as counter electrode and a saturated calomel electrode as reference electrode, the latter separated from the working electrode compartment by a closed electrolyte bridge to prevent chloride contamination.The potentials in this work are referred to that of the reversible hydrogen electrode. The electrolyte solutions were either 0.5 M H_2SO_4 or 1.0 M $HClO_4$. The real surface area was determined through the charge required for adsorbed hydrogen monolayer formation.

Current potential curves at different rotation rates for ORR were recorded between 1.0 and 0.2 V at 5 mV s^{-1} and at 60 °C.

Table 1 Physicochemical characteristics of Pt and Pt-Fe/C catalysts

Catalyst	Particle size/nm	length A_0/nm	Pt/Me at. (XRF)
60%Pt/C	2.8	0.392	-
60%Pt-Fe/C	2.4	0.390	3.33

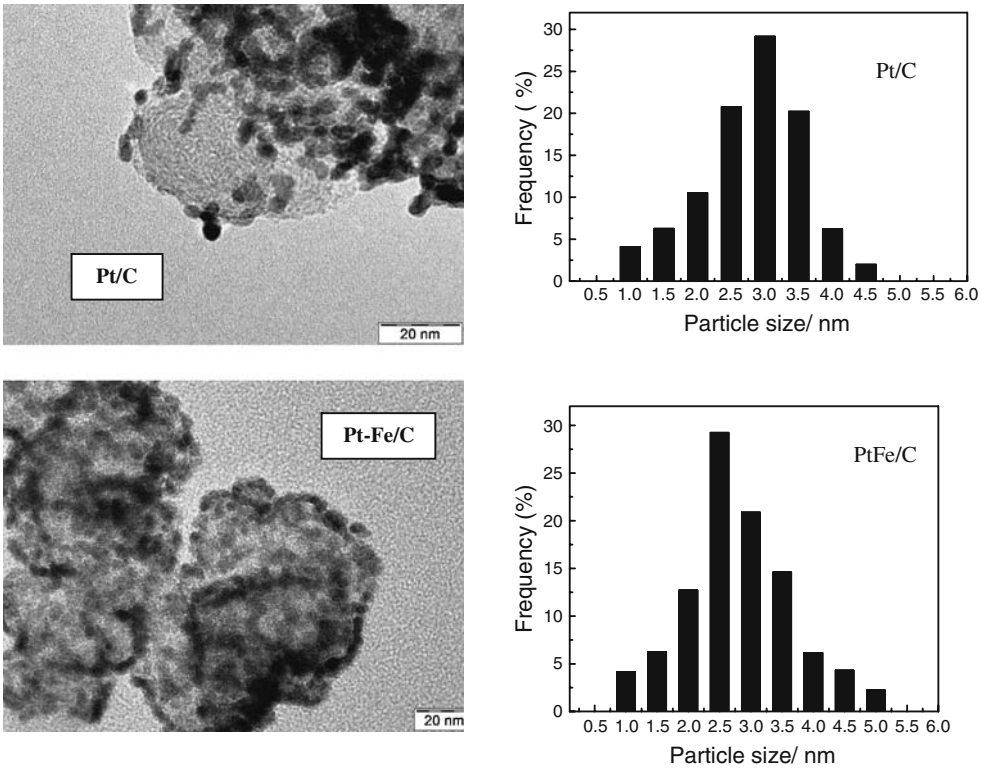

Fig. 2 TEM images and histograms of particle size distribution for 60% Pt and 60% Pt-Fe/C catalysts

Kinetically controlled currents at each potential in the potential region corresponding to a mixed control (diffusion + activation) were obtained through Levich–Koutecky plots. The Nafion® film used in the rotating disc electrode does not offer any diffusion contribution, and it can be neglected as a term in Koutecky–Levich equation.

Results and discussion

Physicochemical characterisation

XRD patterns of Pt/C and Pt–Fe/C catalysts are shown in Fig. 1. They confirm the typical *fcc* structure of Pt and its

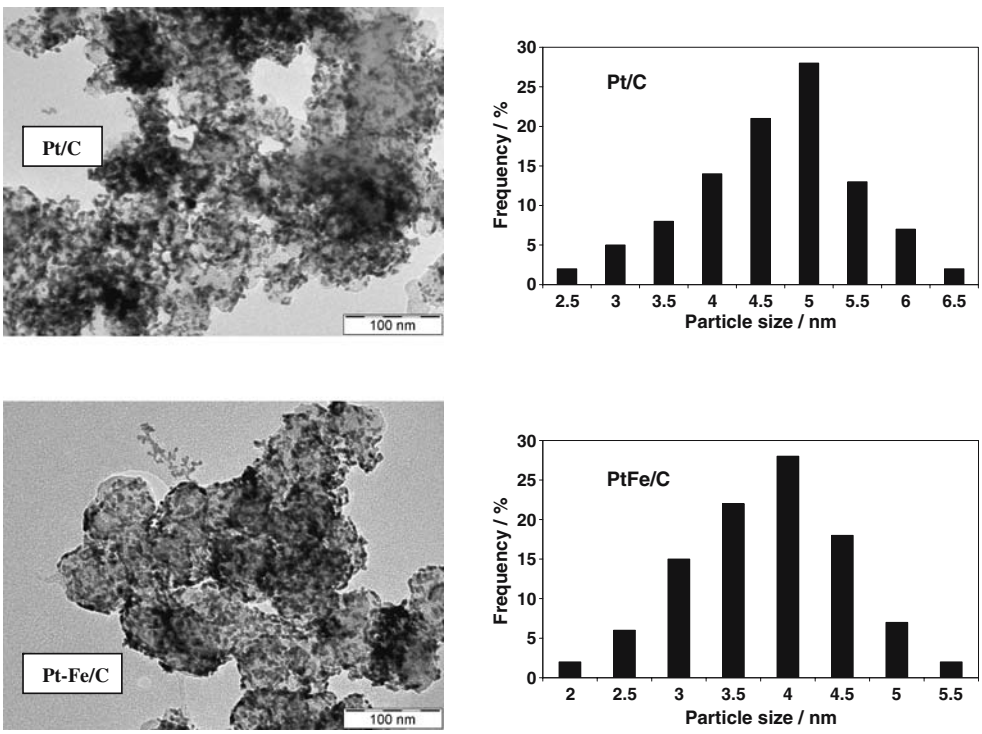

Fig. 3 TEM images at low magnification and histograms of particle size distribution for 60% Pt and 60% Pt-Fe/C electrodes after electrochemical testing

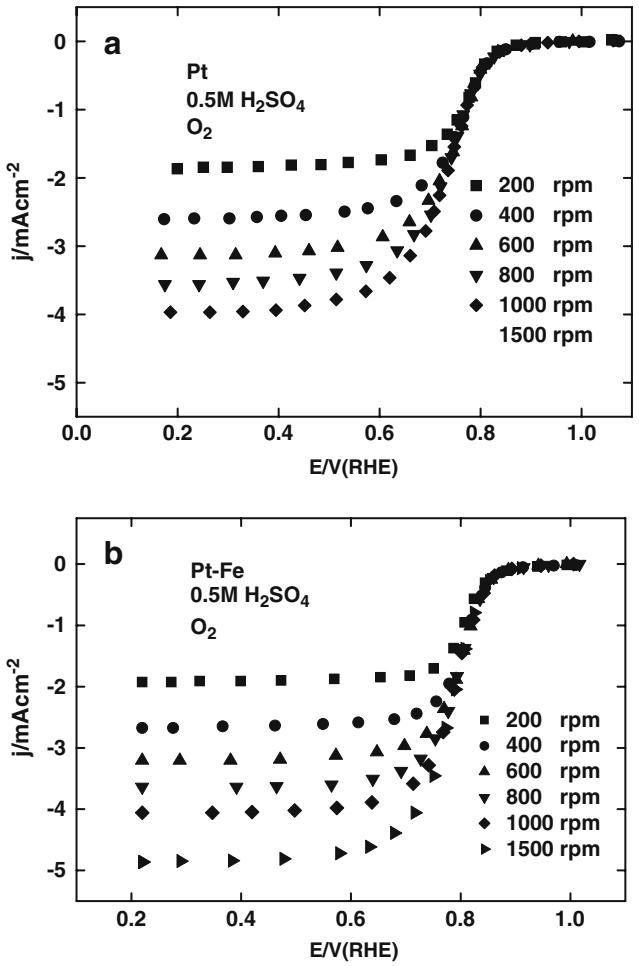

Fig. 4 **a**) Polarisation curves in 0.5 M H_2SO_4 at different disc rotation rates for ORR a) on Pt and **b**) on Pt-Fe

alloys. A moderate degree of alloying was found for the Pt–Fe catalyst, as indicated by a slight shift of the X-ray diffraction peaks to higher Bragg angles. Particle dimensions of 24 and 28 Å were obtained for the Pt–Fe alloy and Pt catalyst, respectively.

The physicochemical characteristics of the catalysts are presented in Table 1.

The data reported in Table 1 show a moderate degree of alloying of Fe with Pt as indicated by the slight decrease in the lattice parameter. Taking into account that chemisorption of oxygen on the electrocatalysts is the first step of the ORR, the geometrical influence of the Pt lattice constant is quite significant for the overall reaction, a contraction of Pt lattice constant facilitates the dissociative O_2 adsorption, and the catalyst binds more strongly atomic oxygen [19]. Nevertheless, it has been previously shown in the literature that Pt–Fe catalysts with small lattice constant contraction show a significant enhancement of the electrocatalytic activity for ORR [20].

The lattice constant contraction obtained using this low temperature preparation route is small compared to Pt–Fe catalyst obtained by carbothermal reduction at high temperatures [21]. Although a large contraction in Pt–Fe lattice is favourable in terms of specific activity, recent studies have shown that intermediate reduction temperatures, resulting in small Pt–Fe lattice contraction, are associated with a mass activity significantly higher than bare Pt catalysts [21].

TEM analysis of the catalysts before and after operation (Figs. 2 and 3) shows a homogeneous distribution of fine metal particles on Vulcan support; this may be clearly observed in the TEM pictures of Pt and Pt- and Fe-based electrodes at low magnification after the electrochemical testing (Fig. 3). A slight increase in the particle size is observed after the electrochemical experiments, indicating that a small electrochemical sintering occurs during the electrochemical analysis. The particle size distribution histograms for both catalysts are also shown in Figs. 2 and 3. The mean particle size of the Pt catalyst increases after the electrochemical testing from 3 to 5 nm, whereas in the Pt–Fe catalyst, the average particle size in the electrode is about 4 vs 2.5 nm in the raw powder.

Electrochemical characterisation

Rotating disc polarisation curves

Typical polarisation curves for ORR on the Pt/C and Pt–Fe catalyst catalysts in 0.5 M H_2SO_4 at 60 °C for disc rotation rates (ω) varying from 200 up to 1,500 rpm are shown in Fig. 4a and b.

The electrocatalytic activity of the Pt/C catalyst appears comparable to that reported in the literature for state-of-the-art commercial catalysts in similar RDE experiments [22].

The oxygen reduction reaction is diffusion-limited at $E<$ 0.6 V. A shift towards more positive potentials values in the

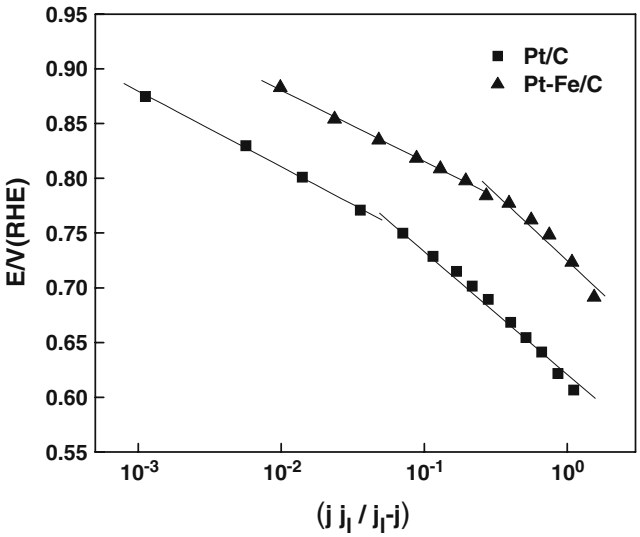

Fig. 5 Tafel plots for ORR on Pt and PtFe catalysts in 0.5 M H_2SO_4

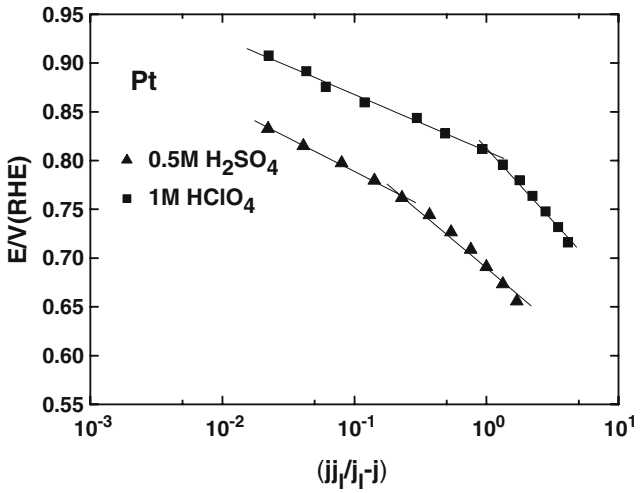

Fig. 6 Tafel plots for ORR on Pt/C in 0.5 M H_2SO_4, and 1 M $HClO_4$

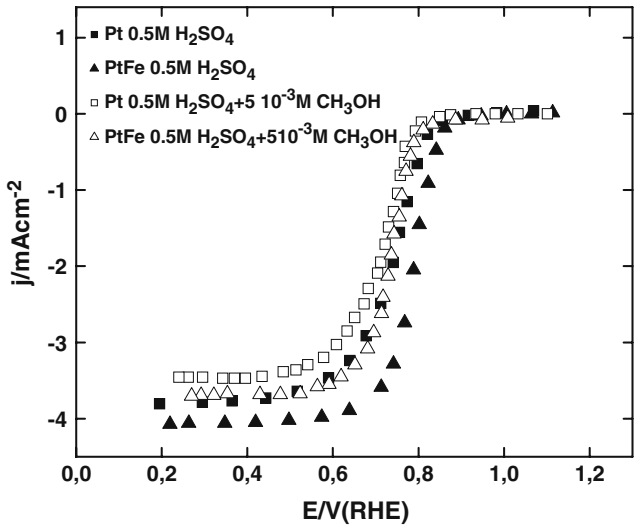

Fig. 8 Polarisation curves at 1000 rpm for ORR in 0.5 M H_2SO_4 with and without 0.005 M CH_3OH, on Pt and Pt-Fe catalysts

onset potential for the ORR on Pt–Fe is observed, indicating a better electrocatalytic activity vs bare Pt. The presence of a Pt skin over the alloy together with an electronic effect induced by Fe on Pt was previously reported by Toda et al. [9] to explain the enhanced catalytic activity for Pt–Fe catalysts. The formation of the Pt skin probably occurs because iron on the surface leaches out of the alloy during operation in acidic electrolytes, while Pt atoms are redeposited and rearranged on the surface. For what concerns the electronic effect, it was emphasised that the electronic structures of the Pt skin layers are altered by the underlying alloy substrates, which, in turn, facilitate the electron transfer to oxygen molecules [9].

On the other hand, Wenzhen Li et al. claimed that the improvement in the performance of Pt–Fe/C for ORR may be partly due to the higher peroxide decomposition activity of Pt in presence of dissolved Fe favouring the 4 e^- transfer route [20]. In this respect, XPS measurements showed a decrease in Fe contain, revealing a partial ion dissolution during the work [23].

Assuming that the kinetics at the rotating disc is mainly activation-controlled in the range $0.6<E<0.9$ V, the associated Tafel plot, [E vs $\log(j_k)$], where j_k is the kinetic current density, can be depicted after mass transport correction in the liquid electrolyte. The kinetic current density j_k, at constant E and ω, was calculated from the equation: $j_k(E,\omega) = (j * j)/(j_l - j)$, where j and j_l are the measured and the corresponding limiting current density, respectively. Tafel plots for ORR on Pt and Pt–Fe are shown in Fig. 5.

The j and j_l values are taken from the polarisation curve at 1,000 rpm. Two linear regions are clearly determined,

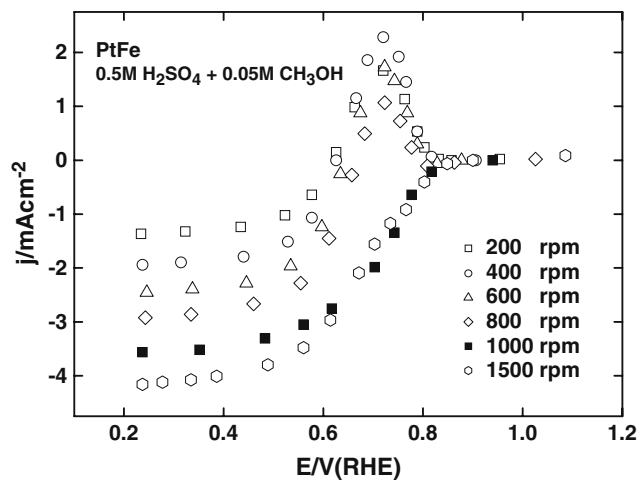

Fig. 7 Polarisation curves at different ω, for ORR in 0.5 M H_2SO_4 + 0.05 M CH_3OH on PtFe

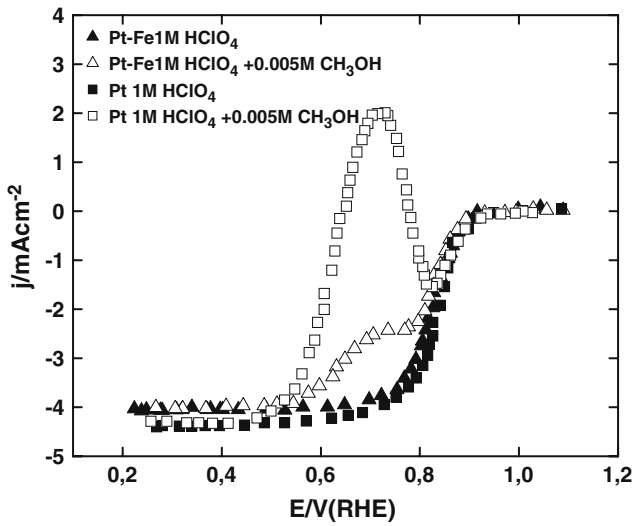

Fig. 9 Polarisation curves at 1000 rpm for ORR in 1 M $HClO_4$ with and without 0.005 M CH_3OH, on Pt and Pt-Fe catalysts

one in the oxide region, i.e. $E>0.75$ V, with a slope of ca RT/F, and the other in the free oxide region for $E<0.75$ V, with a slope of ca 2RT/F.

It is interesting to emphasise that the polarisation curve for ORR on Pt employing supporting electrolyte with different anions, i.e. 0.5 M H_2SO_4 or 1 M $HClO_4$, also exhibits an anodic shift in the onset potential for the electrolyte with a less adsorbable anion such as ClO_4^- (Fig. 6). The HSO_4^- anions forms an ordered bisulphate adlayer on Pt (111) that hinders the ORR, whereas the weakly adsorbed ClO_4^- does not influence the reaction kinetics as described by Macia et al. [14].

The effect of anions is quite similar to that found by Murthi et al. [24] for high concentrated CF_3SO_3H that reported a high ORR activity on an oxide-free Pt surface under conditions of low water activity.

Experiments run with Pt or Pt–Fe catalysts in acid solutions with methanol in concentrations varying from 0.005 to 0.5 M show the loss in catalyst performance for ORR in the presence of methanol. On the electrode surface occurs simultaneously the oxygen reduction and the methanol oxidation, and the overall process is a combination of both reactions leading to the formation of a mixed potential. However, the effective current is not a simple algebraic sum of oxygen reduction and methanol oxidation currents as recently reported by Jusys and Behm [25].

The loss in catalytic performance is more evident either by increasing methanol concentration or by lowering the disc rotation rate (Fig. 7). It must also be emphasised that the solubility value of O_2 in H_2SO_4 at 60 °C is ca 8 10^{-4} M, and the methanol concentration ranges between 5 10^{-2} and 5 10^{-3} M.

The influence of methanol on Pt and Pt–Fe catalyst performance for ORR in 0.5 M H_2SO_4 with and without methanol is shown in Fig. 8. Both catalysts exhibit an increase in overpotential in the presence of methanol. Furthermore, it can also be observed that Pt–Fe maintains a higher catalytic activity than Pt catalyst for ORR in the presence of methanol.

The polarisation curves for ORR on Pt and Pt–Fe in 1 M $HClO_4$ with and without methanol reported in Fig. 9 show that despite the similar catalytic activity of both catalysts for ORR in the absence of methanol, the Pt–Fe catalyst exhibits a higher methanol tolerance in the supporting electrolyte with less adsorbable ions. The better performance of Pt–Fe catalyst in sulphuric acid solution compared to that in 1 M $HClO_4$ (Fig 9), both in the presence of methanol, indicates that the adsorbed bisulphate anions play an important role in protecting the electrode from methanol poisoning.

It is also important to point out that an improvement in DMFC single cell performance has been observed when the cell was equipped with a Pt–Fe cathode catalyst instead of a Pt/C catalyst [16]. A maximum power density of 87 mW cm^{-2} was obtained under similar conditions, but with air feed at the cathode instead of oxygen. This indicates a higher electrocatalytic activity of the bimetallic phase towards the oxygen reduction reaction and a larger tolerance towards the poisoning effects of methanol crossover.

Conclusions

A Pt–Fe catalyst with a particle size of less than 3 nm and with a small degree of alloying was synthesised using a colloidal preparation procedure. An enhancement in the ORR kinetics in 0.5 M H_2SO_4 with and without methanol was observed on the Pt–Fe alloy as compared to Pt. The ORR and methanol tolerance appears to be influenced by electrolyte composition. The adsorbed bisulphate anions from the electrolyte seem to play an important role in protecting the electrode from methanol poisoning.

Acknowledgements The authors gratefully acknowledge financial support from MAE-SeCyT Cooperation Programme; (2004-2005), CONICET and Agencia Nacional de Promoción Científica y Tecnológica of Argentina and from “Regione Piemonte” (Italy) through the Micro Cell project (Delibera della Giunta Regionale no. 25-14654 del 31/01/05). AMCL acknowledges International Cooperation support from CIC de la Provincia de Buenos Aires.

References

1. Aricò AS, Srinivasan S, Antonucci V (2001) Fuel Cells 1:133
2. Ren X, Wilson MS, Gottesfeld S (1996) J Electrochem Soc 143:L12
3. Salgado JR, Antolini E, Gonzalez ER (2005) Appl Catal B Environ 57:283
4. Koffi RC, Coutanceau C, Garnier, Leger JM, Lamy C (2005) Electrochim Acta 50:4117
5. Paulus UA, Wokaun A, Scherer, GG, Schmidt TJ, Stamenkovic V, Radmilovic V, Markovic NM, Ross PN (2002) J Phys Chem B 106:4181
6. Mukerjee S, Srinivasan S, Soriaga MP, Mc Breen JM (1995) J Electrochem Soc 142:1409
7. Mukerjee S, Srinivasan S (1993) J Electroanal Chem 357:201
8. Pourbaix M (1966) Atlas of electrochemical equilibria in aqueous solutions. Pergamon, New York
9. Toda T, Igarashi H, Uchida M, Watanabe M (1999) J Electrochem Soc 146:3750
10. Castro Luna AM, Camara GA, Paganin VA, Ticianelli EA, Gonzalez ER (2000) Electrochem Commun 4:222
11. Yu P, Pemberton M, Plasse P (2005) J Power Sources 144:11

12. Médard C, Lefevre M, Dodelet JP, Jaouen F, Lindbergh G (2006) Electrochim Acta 51:3202
13. Zinola CF, Castro Luna AM, Triaca WE, Arvia AJ (1994) J Appl Electrochem 24:119
14. Macia MD, Campiña JM, Herrero E, Feliu JM (2004) J Electroanal Chem 564:141
15. Kinoshita K (1990) J Electrochem Soc 137:845
16. Baglio V, Arico AS, Stassi A, D´Urso C, Di Blassi A, Castro Luna AM, Antonucci V (2007) J Power Sources (in press)
17. Petrow HG, Allen RG (1976) US Pattern 3992:331
18. Paulus UA, Schmidt TJ, Gasteiger HA, Behm RH (2001) J Electroanal Chem 495:134
19. Xu Y, Ruban A, Mavrikakis M (2004) J Am Chem Soc 126:4717
20. Li W, Zhou W, Li H, Zhou Z, Zhou B, Sun G, Xin Q (2004) Electrochim Acta 49:1045
21. Min M, Cho J, Cho K, Kim H (2000) Electrochim Acta 45:4211
22. Schmidt TJ, Paulus UA, Gasteiger HA, Behm RJ (2001) J Electroanal Chem 508:41
23. Stassi A, D'urso C, Baglio V, Di Blasi A, Antonucci V, Arico AS, Castro Luna AM, Bonesi A, Triaca WE (2007) J Appl Electrochem (in press)
24. Murthi V, Urian RC, Mukerjee S (2004) J Phys Chem B 108:11011
25. Jusys Z, Behm RJ (2004) Electrochim Acta 49:3981